Behavior of Cellulose Liquefaction After Pretreatment Using Ionic Liquids with Water Mixtures

Qingyue Wang, Qiyu Chen, Naoki Mitsumura, Sarkar Animesh

Department of Environmental Science and Technology, Graduate School of Science and Engineering, Saitama University, Saitama city, Saitama 338–0825, Japan
Correspondence to: Q. Wang (E-mail: seiyo@mail.saitama-u.ac.jp)

ABSTRACT: Ionic liquid (IL)-water mixtures were applied in cellulose pretreatment experiment and the pretreated cellulose was used in subsequent phenol liquefaction process as a new application method. Cellulose recovery rate and the average molecular weight (M_w) of pretreated cellulose were investigated to understand the influence of these mixtures on cellulose structure. X-ray diffraction, Fourier transform infrared, gel permeation chromatograph, and scanning electron microscope were used to clarify the changes of pretreated cellulose. The liquefied residues from untreated cellulose and pretreated cellulose were considered as significant index to determine the effect of IL-water mixtures on cellulose. Moreover, liquefied residues were initially characterized by the variation of the average M_w. It was suggested that the lower M_w of cellulose obtained in IL-water mixtures, and the crystalline structure was disrupted. So, some cracks were found on the cellulose surface obviously. The liquefied residues result suggested that the pretreated cellulose obtained the lower residues at the same time or the same amount of residues by using the less time. The behavior of cellulose liquefaction efficiency using IL-water mixture pretreatment was discussed. The lower M_w of cellulose was the major factor, which accelerates the cellulose phenol liquefaction process efficiency. © 2014 Wiley Periodicals, Inc. J. Appl. Polym. Sci. **2014**, *131*, 40255.

INTRODUCTION

Liquefaction technology is one of the effective chemical methods to use the biomass resources. The liquefied products were used for the preparation of different biomass-based polymers materials. Lin had attempted to explain the liquefaction reaction mechanism of cellulose with phenol solvent under the acid-catalyzed conditions.[1] It was found that the yields of various products could be depended on the reaction conditions. As the target products, biomass-base polyurethane material and Novolak PF resins were prepared, and its structures and properties were discussed.[2,3] However, the biomass-based polymer materials had not widely applicable due to some problems. Initially, condensation reaction was occurred if the liquefaction experimental conditions changed in the cellobiose study (such as solvent/cellulose addition ratios).[4] An early study was also reported that the insoluble residue was formed when cellulose and lignin coexisted.[5] Thus, the mechanism of forming the condensed residues during the liquefaction process needs to be clarified.[6] Secondly, it needs to drive the research to overcome the problems with drawbacks of physical and mechanical properties of resin products.[7] Moreover, it was inefficient to liquefy the biomass of higher crystallinity index such as bamboo with a longer reaction time.[8] This long reaction

time considerably increases the product cost of biomass-based products and consequently hinders future commercialization efforts. Ozone treatment was discussed as one of the improvement methods where the amorphous cellulose was decomposed during the treatment processes in order to lead cellulose liquefaction more efficiently.[9] However, ozone treatment method would cause new pollution.

Ionic liquids (ILs) were claimed as "green solvents" and possible alternative of volatile organic solvents.[10] Since Rogers and coworkers reported that cellulose could dissolve in ILs,[11] many studies had been focused on the subject of lignocellulosic biomass conversion which examined the amount of cellulose solubility in ILs.[12] ILs also attracts interest in applications. Lignocellulosic biomass could convert the composition into biofuel or chemicals by different ILs pretreatment processes for the declining fossil fuel resources.[13–15] Moreover, ILs as biomass pretreatment solvents have been attracted attention in the field of sugars.[16,17] But, it is hard to apply ILs independently in the field of biotechnology for biofuel or chemicals due to the high cost.

Water is the most abundant fluid; ILs-water mixture should be capable of acting as functional fluids in bioscience and for
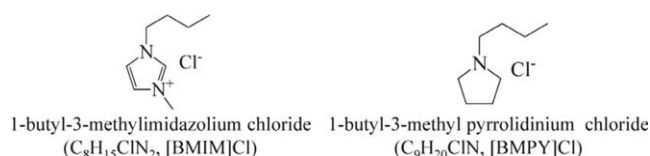
1-butyl-3-methylimidazolium chloride
(C$_8$H$_{15}$ClN$_2$, [BMIM]Cl)

1-butyl-3-methyl pyrrolidinium chloride
(C$_9$H$_{20}$ClN, [BMPY]Cl)

Figure 1. The molecular structures of ILs used in this study.

large-scale usage of biomass during the pretreatment step.[18,19] It was found that selected ILs with water mixture was effective in enhancement of cellulose digestibility.[20,21] Thus, the potential use of ILs-water mixture solvent for a new application in the field of biomass solvent liquefaction could be expected.

In this study, cellulose was pretreated by ILs including [BMIM]Cl-water and [BMPY]Cl-water mixture with or without solid acid catalysis. Then, the pretreated cellulose was used in subsequent phenol liquefaction process. The effect of mixtures on pretreated cellulose was characterized by Fourier transform infrared (FT-IR) spectroscopy, X-ray diffraction (XRD), gel permeation chromatography (GPC), thermo gravimetric/differential thermal (TG-DTA), and scanning electron microscope (SEM) analysis. A liquefied residue from the untreated cellulose and pretreated one has been studied for its potentiality in liquefaction process. This study aimed to explore the use of ILs-water mixture pretreated cellulose as raw materials to observer its behavior in the liquefaction reaction process.

MATERIALS AND METHODS

Materials and Chemicals

Microcrystalline cellulose (MCC) powder was supplied by Sigma-Aldrich. The cellulose powder was dried in oven at
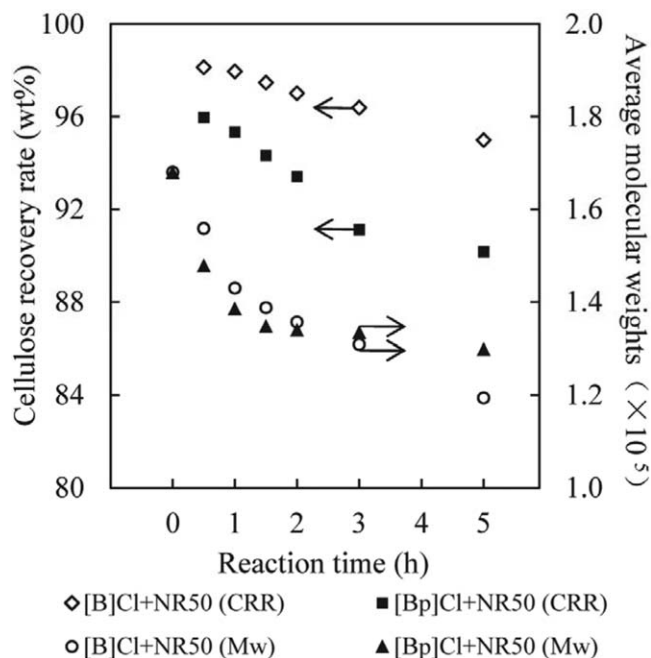

Figure 2. CRR and average M_ws of sample. The pretreated cellulose was prepared for nitrocellulose to determine the M_ws. The sample code could refer to Table III.
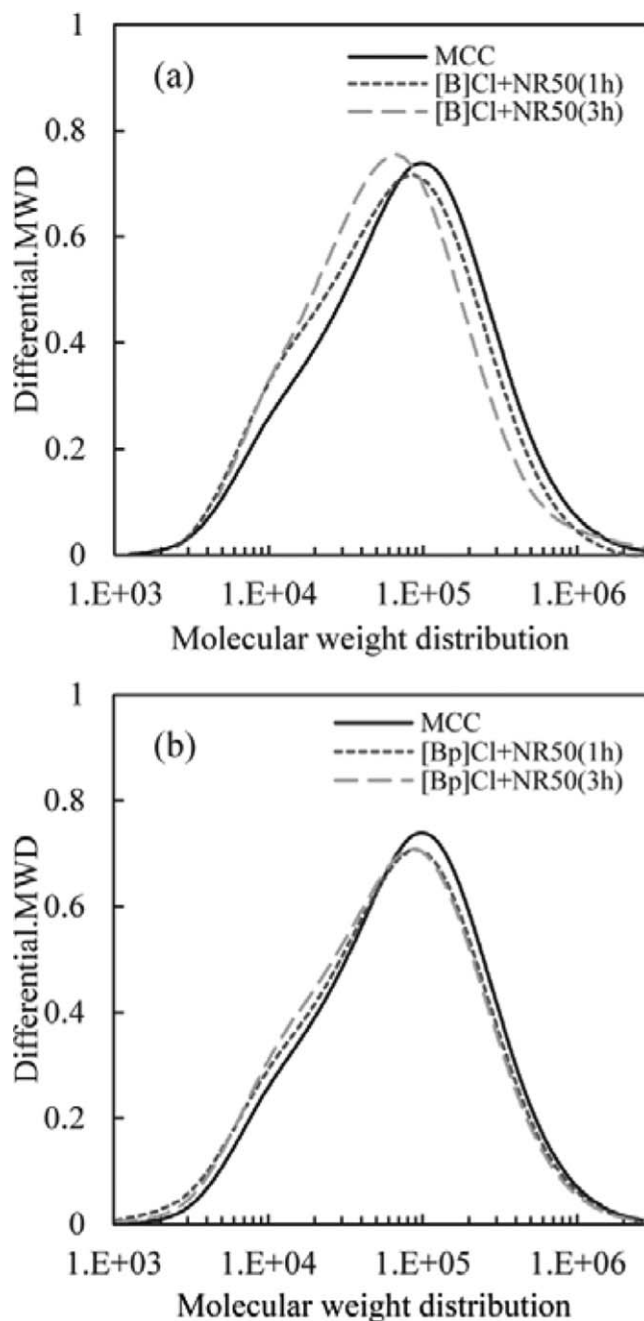

Figure 3. M_w distribution of MCC and pretreated cellulose (nitrocellulose) with different pretreatment condititon. (a) pretreated by [BMIM]Cl-water mixture and (b) pretreated by [BMPY]Cl-water mixture.

105°C for 24 h before using. The molecular structures of ILs were summarized in Figure 1, 1-butyl-3-methylimidazolium chloride (C$_8$H$_{15}$ClN$_2$, [BMIM]Cl; sample code [B]Cl) and 1-butyl-3-methyl pyrrolidinium chloride (C$_9$H$_{20}$ClN, [BMPY]Cl; sample code [Bp]Cl) were purchased from the Wako (Pure Chemical Industries, Japan). Polymer catalysis Nafion®NR50 (NR50) was purchased from Sigma-Aldrich. Phenol was used as the liquefaction solvent. Sulfuric acid (95%; SA) was used as the acid catalyst. All chemicals in this study were reagent grade and were used without further purification.
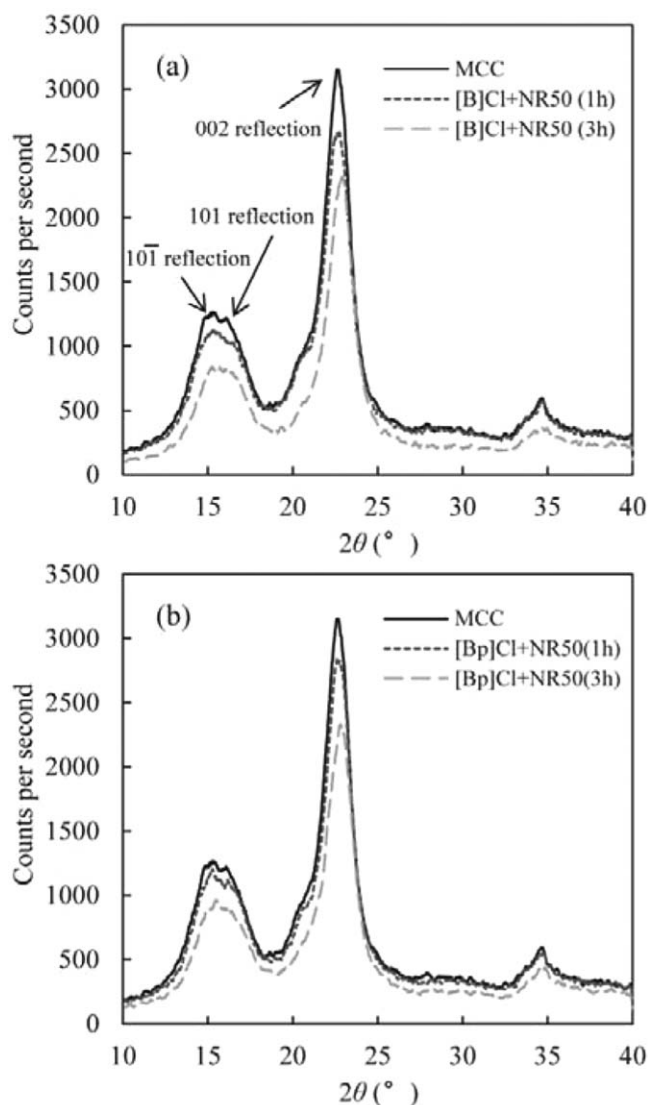
Figure 4. The XRD result of MCC and pretreated cellulose with different pretreatment conditions. (a) pretreated by [BMIM]Cl-water mixture and (b) pretreated by [BMPY]Cl-water mixture.

Table I. Parameters Obtained from the XRD Analysis of Pretreated Samples

	$d_{10\bar{1}}$ (Å)	d_{101} (Å)	d_{002} (Å)	Amorphous 2θ	Apparent Cr.l
MCC	5.90	5.60	4.03	18.32	79.4
[B]Cl + NR50 (1 h)	5.89	5.56	4.02	18.50	85.4
[B]Cl + NR50 (3 h)	5.88	5.50	3.97	18.52	84.5
[B]Cl + NR50 (5 h)	5.86	5.54	3.98	18.56	83.3
[Bp]Cl + NR50 (1 h)	5.87	5.57	4.02	18.50	84.6
[Bp]Cl + NR50 (3 h)	5.86	5.56	4.02	18.50	83.1
[Bp]Cl + NR50 (5 h)	5.87	5.55	3.99	18.58	81.6

Liquefaction of Cellulose

The liquefaction process was performed in a 20 mL round bottle. The neck flask equipped with refluxing condenser, was immersed in an oil bath at 120 or 150°C and magnetic stirring was used at 1000 rmp/min rotating speed. The mixing ratio of ILPC or untreated cellulose and phenol was set to 1 : 4. The amount of SA was taken 10 or 20 wt % of the total weight of phenol solvent as the acid catalyst. The liquefied residue was dried in an oven at 105°C for 24 h and the rate calculated by eq. (2).

$$\text{Residue rate (wt \%)} = (W_r/W_i) \times 100 \qquad (2)$$

where, W_i: the weight of samples before liquefaction; W_r: the weight of liquefied residue after dried in oven.

Pretreatment of Cellulose

MCC was added into a flask containing amount of ILs and deionized water with or without solid acid (MCC/ILs/NR50, 1/10/1 was set to weight ratio; ILs/water, 1/10 was set to molar ratio). Pretreatment materials was heated and stirred in flask by oil bath at 100°C for 1–5 h. To remove the mixtures from the pretreated cellulose, all the samples were washed by methanol and deionized water three times, respectively. The pretreated cellulose was filtered on a No. 40 filter paper (Whatman G.E., Co.) and dried in oven at 105°C for 24 h. The solubility of cellulose in IL has been calculated the eq. (1):

$$\text{Cellulose recovery rate (CRR, wt \%)} = (W_p/W_i) \times 100 \qquad (1)$$

where, W_i: the weight of dried cellulose before pretreatment; W_p: the weight of pretreated cellulose after dried in oven.
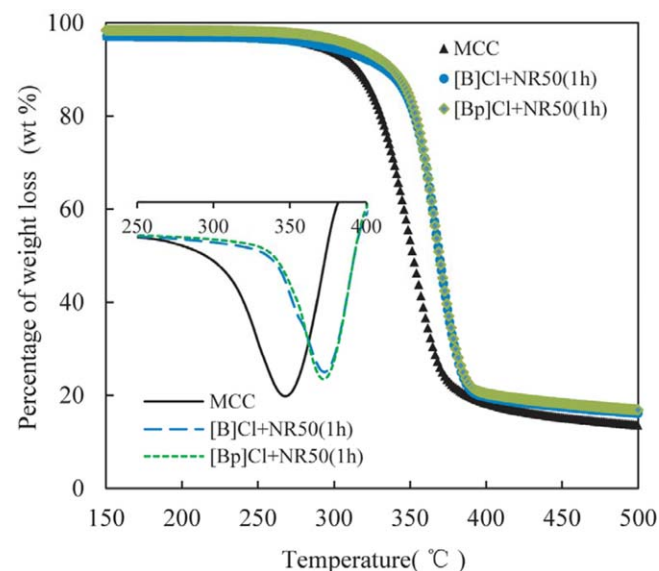

Figure 5. The TG-DTA result of MCC, [B]Cl + NR50, and [Bp]Cl + NR50 sample. [Color figure can be viewed in the online issue, which is available at wileyonlinelibrary.com.]

Table II. Thermal Decomposition Characteristic Parameters of MCC, [B]Cl + NR50, and [Bp]Cl + NR50 Sample

Sample code	Δw (%)[a]			T_{DTGmax} (°C)[b]
	400°C	600°C	800°C	
MCC	18.4	16.9	13.8	345
[B]Cl + NR50	20.4	18.2	17.0	375
[Bp]Cl + NR50	20.5	18.4	17.1	378

[a] Mass loss.
[b] Temperature at maximum rate of mass loss.

GPC Analysis

The nitrocellulose was prepared to evaluate the average molecular weight (M_w) of cellulose. The nitrocellulose was dissolved in THF with the ratio of 0.1% (w/v) and filtered through a 0.45 μm membrane. The M_w distribution was determined by a GPC system equipped with KD806L gel columns (Shodex, Showa Denko K.K., Japan) for nitrocellulose; equipped with both KD-802 (Shodex, Showa Denko K.K., Japan) and KD806L for liquefied products in a series at 40°C. The average M_w of the samples were calculated by Jasco-Borwin software and using a calibration curve of monodisperse polystyrene standards (M_w = 1,260,000, 710,000, 355,000, 43,900, 9500, 2800, 945, and 550, which were made the standard curve for nitrocellulose samples; M_w = 21,800, 13,000, 10,400, 6940, 4910, 2940, 2170, 1280, 770, and 580 were made the standard curve for liquefied products). Tetrahydrofuran (THF) solution was used as eluent and the flow rate was 1.0 mL/min.

XRD Analysis

Crystalline structures of pretreated cellulose and liquefied residue were analyzed by an Ultima III X-Ray diffractometer (Rigaku, Japan). Ni-filtered Cu $K\alpha$ radiation (λ = 0.1542 nm) was generated at 40 kV voltage and 40 mA current. Intensities range was from 10° to 40° with 2°/min scan speed for total XRD analysis experiment. The crystallite height 002 (I_{002}) and amorphous height (I_{am}) were used to calculate the crystalline index (Cr.I.) and was calculated by the eq. (3). The apparent crystallite size (L) of the refection of plane was calculated from the Scherrer equation based on the width of the diffraction patterns by the eq. (4). The surface chains occupy a layer ~0.57 nm thick so the proportion of crystallite interior chains was

calculated by the eq. (5), the interlayer distances (d) was calculated by eq. (6).

$$Cr.I. = (I_{002} - I_{am})/I_{002} \times 100 \qquad (3)$$

$$\text{Crystallite size } (L) = (K \times \lambda)/(\beta \times \cos\theta) \qquad (4)$$

where, K, the Scherrer constant of value 0.94; λ, the X-ray wavelength (0.1542 nm); β, the half-height width of the diffraction band; θ, the Bragg angle corresponding to the (002) planes.

$$\text{Crystallite interior chains } X = (L - 2h)^2/L^2 \qquad (5)$$

where, L, the apparent crystallite size for the refection of plane (002); h, the layer thickness of the surface chain is 0.57 nm.

$$\text{Interlayer distances } d = \lambda/2\sin\theta \qquad (6)$$

where, λ, the X-ray wavelength (0.1542 nm); θ, the Bragg angle corresponding to the (101, 101, or 002) planes.

FT-IR Spectrometer Analysis

Pretreated cellulose was analyzed by FT-IR spectrometer (Model IR-6100, Jasco, Japan). The ratio of samples and spectroscopic grade KBr was 1 : 100; all of the infrared spectra were recorded in absorbance units within the range of 4000–400 cm^{-1}.

SEM Analysis

The surface morphological changes of cellulose, pretreated cellulose, and liquefied residue were observed to understand the pretreatment process by a SEM (Model S-2400, Hitachi, Japan) under an acceleration voltage of 15kV.

Thermo Gravimetric/Differential Thermal Analysis (TG-DTA)

Untreated cellulose and pretreated sample were analyzed by the TG-DTA (Model DTG-60, Shimadzu, Japan) under the following conditions: about 20 mg of samples were heated at a rate of 10°C min^{-1} starting from room temperature until 900°C. A gas flow rate of 250 mL min^{-1} was used.

RESULTS

Characteristic of IL Pretreated Cellulose Samples

In ILs–water pretreatment process, water molecules were bound with two anions by forming a symmetric complex hydrogen bond.[22] Thus, water prevents ILs to dissolve the cellulose and impair ILs function in pretreatment step, but the mixtures can affect of cellulose on the physical and chemical properties.[13,15] Taking into account this point, in this study, solid acid catalysis was added in the mixture to promote the activity of mixture system.

Table III. The Apparent Cr.I and Average M_w of IL Pretreated Cellulose Samples

Sample code	Treatment conditions		Apparent Cr.I	M_w[a]
	IL	Catalysts		
MCC	–	–	76	1.6E + 05
[B]Cl	[BMIM]Cl	–	78	1.5E + 05
[B]Cl + NR50	[BMIM]Cl	Nafion®NR50	81	1.3E + 05
[Bp]Cl	[BMPY]Cl	–	77	1.5E + 05
[Bp]Cl + NR50	[BMPY]Cl	Nafion®NR50	85	1.3E + 05

[a] The average M_w of nitrocellulose preparation of 3 h pretreated sample.
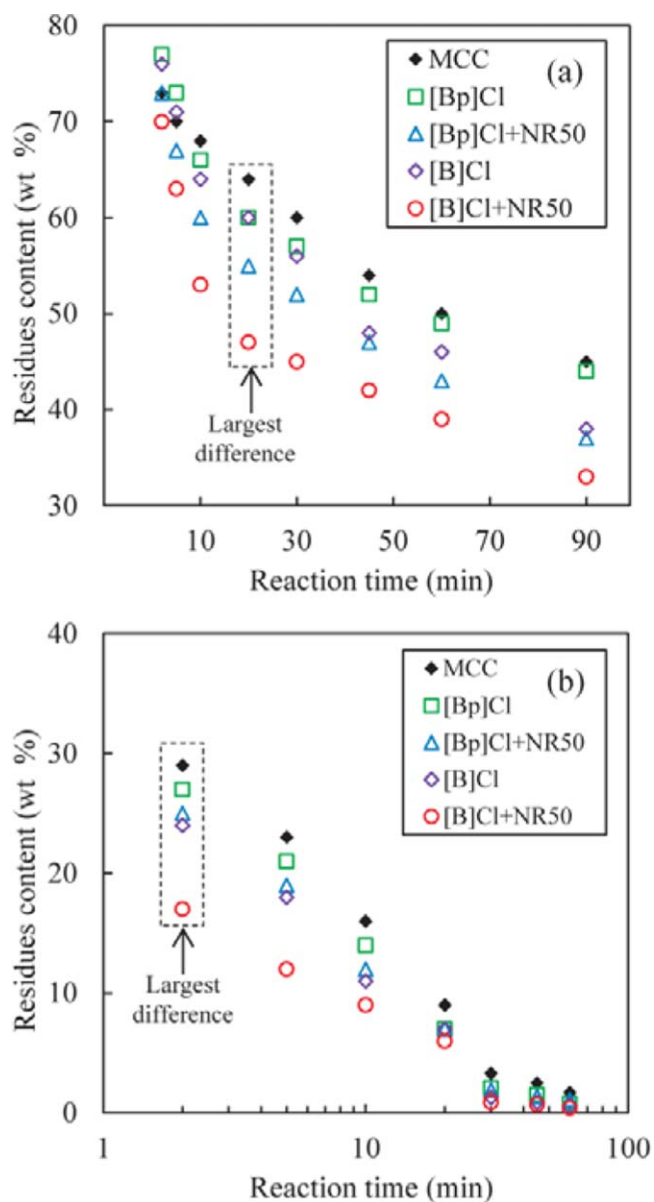
Figure 6. The residues content of MCC and pretreated cellulose with different liquefaction condition. (a) Liquefaction temperature: 120°C, sample/phenol/SA, 1/4/0.4; (b) Liquefaction temperature: 150°C, sample/phenol/SA, 1/4/0.8. The largest difference of residues content was described in the dotted box. [Color figure can be viewed in the online issue, which is available at wileyonlinelibrary.com.]

The pretreatment of lignocellulose for subsequent applications process can be attributed to find out the variation of CRR, surface structure, crystallinity structure, and degree of polymerization.[23] Figure 2 shown that about 10 wt % cellulose was dissolved in [BMPY]Cl-water mixture solvent with solid acid catalysis at 100°C for 5 h. The CRR from the pretreated cellulose (pretreated by [BMPY]Cl) suggested that these sample was more readily degradable by the ILs-mixture. The CRR value, average M_w of sample [B]Cl +NR50 and [Bp]Cl +NR50 were decreased with the increasing of pretreatment time. This result represented that both high M_w and low M_w part of cellulose were degradable in this pretreatment process and part of lower

M_w cellulose could be dissolved in mixture. However, the average M_w of [Bp]Cl +NR50 sample was not significantly greater than that from [B]Cl +NR50. It indicated that the [BMPY]Cl had the limitations on the degradation of the high M_w part of cellulose.

The nitrocellulose was prepared to evaluate the M_w of pretreated cellulose where nitrocellulose was considered as a soluble substance in THF solvent. The M_w distribution of two ILs-mixtures pretreated cellulose was shown in Figure 3. It was clear that the part of low M_w in [B]Cl+NR50 sample was increased with extending reaction time where the average M_w of [B]Cl at 1, 3, and 5 h were 1.4E + 05, 1.3E + 05, and 1.2E + 05, respectively. The peak was tending to shift to the low M_w distribution. The significant variation did not appear in [Bp]Cl + NR50 sample, especially in low M_w part. From this result, we can mention that the two kinds of cations ILs-mixtures with solid acid catalysis existed distinct dissolution mechanism on cellulose.

The XRD has been used widely to evaluate the crystalline structure of cellulose. Figure 4 depicts the changes in the XRD diffraction spectra of pretreated cellulose as a function of pretreatment time. MCC displayed an expected peak at $2\theta = 22.5°$ corresponding to (002) plane.[24] A clear shallow shoulder peak suggested that the arrangement of cellulose chains were disturbed within the hydrogen-banded sheets. The result from Nafion®NR50 suggested that the raw sample was distorted and transformed into a lower ordered intermediate structure. The peak in plane 002 of [B]Cl + NR50 (3 h) was lower than that of [B]Cl + NR50 (1 h), and MCC. The shoulder peak of [Bp]Cl + NR50 sample was closer to [B]Cl + NR50 sample. With the increase of pretreated time more disturbances took place in hydrogen bond of cellulose. These diffraction pattern changes were consistent with the global decrease of the crystalline structure in cellulose. Moreover, the shift of the (002) plane in [B]Cl + NR50 sample was decreased from 22.58° ($d_{002} = 4.02$ Å) (1 h) to 22.76° ($d_{002} = 3.98$ Å) (5 h), and (002) plane in [Bp]Cl + NR50 sample was decreased from 22.56° ($d_{002} = 4.02$ Å) (1 h) to 22.72° ($d_{002} = 3.99$ Å) (5 h), were summarized in Table I. Thus, part of hydrogen bond was destroyed in cellulose, then, cellulose intermolecular interactions was reduced, therefore the cellulose crystalline structure was distorted as a result by increasing pretreatment time.[25,26] These results demonstrated that ILs-water mixture with solid acid catalysis could disrupted the crystallite structure of cellulose.

The pretreated cellulose was subjected to TG-DTA. The weight loose percentage of the pretreated cellulose with increasing temperature and the rates of degradation has shown in Figure 5. It was observed that the char left after degradation was 13.8% for MCC, 17.1% for [Bp]Cl + NR50 and 17.0% for [B]Cl+NR50. The pretreated cellulose had more char in compare with MCC. The initial thermal decomposition temperature was started from 256°C and the maximum rate of mass loss were exhibited at 378 and 375°C for sample [Bp]Cl + NR50 and [B]Cl + NR50, respectively, where at 345°C for MCC, was present in Table II. The MCC sample showed the lower residue on thermal degradation, which might be attributed to the lowest flexibility of the microfibrils, very fine and smaller crystallite size.[27]
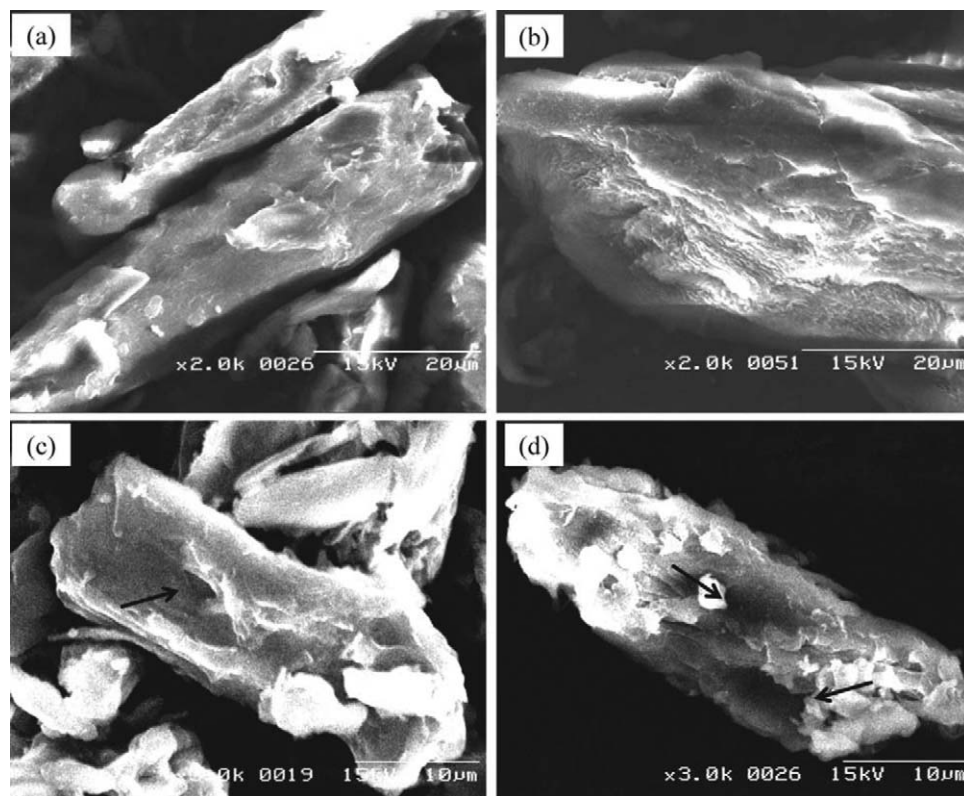
Figure 7. The SEM image of cellulose sample. (a) MCC, (b) [B]Cl + NR50 sample, (c) Liquefied residue from MCC in 15 min, (d) liquefied residue from [B]Cl + NR50 sample in 15 min.

To determine the influence of ILs-water mixture on cellulose liquefaction process, the different ILs cation with $[BMIM]^+$ and $[BMPY]^+$ were used in this study. Apparent Cr.I and average M_w of nitrocellulose, which was prepared from pretreated cellulose were given in Table III. And the increased apparent Cr.I suggested that the amorphous cellulose was dissolved in ILs-water solvent. The nitrocellulose was generally used to evaluate the average M_w of cellulose; the selected ILs could degrade the average M_w of global cellulose. [B]Cl + NR50 and [Bp]Cl + NR50 samples obtained the lower average M_w in compare to the samples [B]Cl and [Bp]Cl, which were used to subsequent phenol liquefaction process.

Effect of Pretreated Cellulose in Liquefaction Process

In phenol or PEG/glycerin solvent liquefaction, some studies were discussed the condensation reactions of liquefied components.[4,28] In this study, liquefaction reaction speed was relatively slow in Figure 6(a), and quick (by rising the reaction temperature and adding more acid catalysis) in Figure 6(b) and avoiding the condensation reactions occurred (ratio of cellulose/phenol <1 : 4).[4] It was clear that the liquefied residue rate from pretreated sample was lower than that in untreated sample and in pretreated sample [B]Cl + NR50 and [Bp]Cl + NR50, the result had obviously lower residue content shown in Figure 6(a). Figure 6(b) represented that samples [B]Cl, [Bp]Cl, [B]Cl + NR50, and [Bp]Cl + NR50 were liquefied by adding 20 wt % SA to observe the behavior of pretreated sample in liquefaction process. The sample [B]Cl + NR50 was liquefied faster than any other sample. It

was interesting that the largest difference result was not occurred in the end of liquefaction process. In the contrast, the largest difference result of liquefied residues were between [B]Cl + NR50 and MCC in Figure 6(a) or [B]Cl + NR50 and MCC in the Figure 6(b), which was happened at the initial stage of the reaction. This result indicated that the effect of pretreatment processes could directly affect the liquefaction speed. Figure 7(a,b) shown some cracks which were observed on the cellulose surface but not on untreated one. Some obvious dimples suggested that the cellulose liquefaction process was irregular shown in Figure 7(c,d).

The liquefied residue was prepared for nitrocellulose to determine the M_w of residue, was present in Figure 8(a). The average M_w value was decreased with the reaction time. The M_w value of MCC, [B]Cl + NR50, and [Bp]Cl + NR50 M_w value were 1.6E + 05, 1.3E + 05, and 1.3E + 05, respectively. The higher M_w value of MCC sample was decreased rapidly at the begging of reaction, and the MCC M_w value was near to the value of [B]Cl + NR50 and [Bp]Cl + NR50 at the end of reaction. The similar variation was also reflected in the results of liquefied product [Figure 8(b)]. The result of M_w value variation from residue samples such as [B]Cl + NR50 and [Bp]Cl + NR50 suggested the liquefaction process behavior of raw sample might due to the lower M_w. Thus, the ILs-water mixture might not affect the internal structure of cellulose particles, but the crystalline structure and the outer surface changed. Moreover, the average M_w value was decreased which was also a significant characteristic for raw sample.[5]
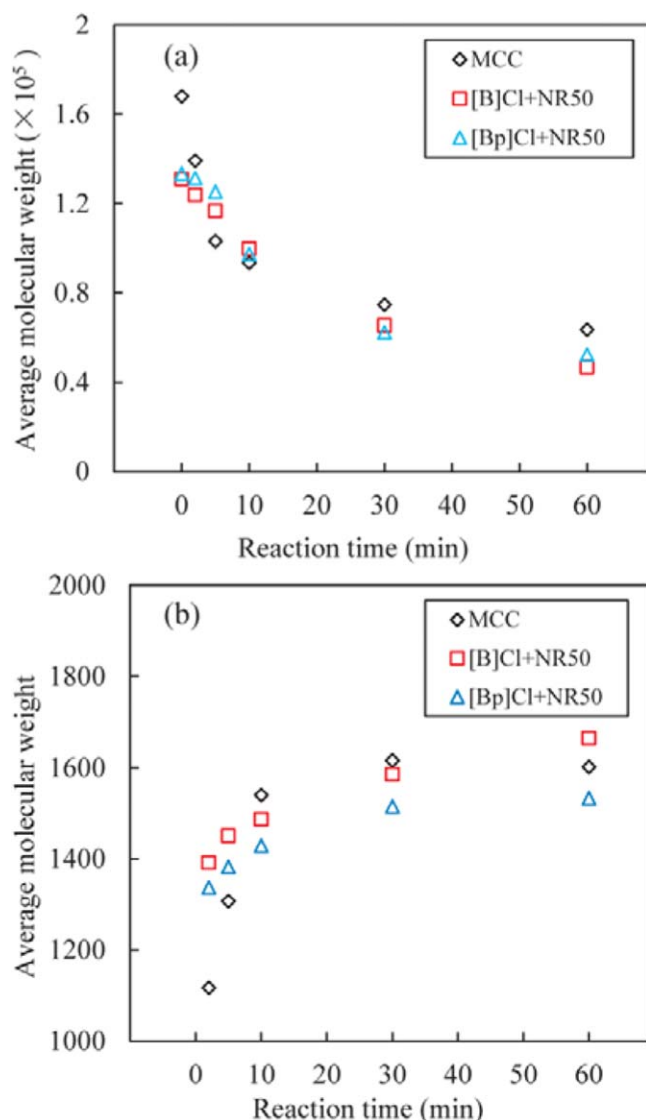
Figure 8. The average M_w of liquefied residue and liquefied products. (a) Nitrocellulose prepared from liquefied cellulose residue, (b) Liquefied products from sample MCC, [B]Cl + NR50, and [Bp]Cl + NR50. The liquefaction condition could refer to Figure 6(b). [Color figure can be viewed in the online issue, which is available at wileyonlinelibrary.com.]

DISCUSSION

MCC powder pretreated by ILs-water mixture has exhibited that the pretreated cellulose could be liquefied efficiently in phenol solvent. To elucidate the affect mechanism of this solvent mixture on cellulose structure, the impact of solid acid catalyst (Nafion®NR50) on pretreated cellulose and the mechanism of liquefaction process were investigated in this study. According to the three points of view, it was clear that MCC was formed by pretreated ILs-water mixtures. First, crystalline structures in cellulose was disrupted significantly; secondly, more lower M_w value of cellulose was determined; thirdly some cracks on cellulose particles (<20 μm) surface structure was observed. Nevertheless, FT-IR spectra in the range of describing hydrogen bonding [inter O(6)H-O(3′); intra O(3)H-O(5) and O(2)H-O(6)] explained the loose crystalline structures caused by break

down of hydroxyl group (data not shown). This suggests that disruption of hydrogen bonds and intrachain structure led to part of lowed M_w value of cellulose dissolved,[29] and the global distribution of M_w move to the lower M_w distribution.

Brandt suggested that water hydrogen-bonds strongly to the IL anion, so reducing their propensity to interact with the cellulose. It also prevents the coordination of IL anions to the cellulose.[30] In this study, the CRR value and average M_w were dropped with the increasing of pretreated time. It indicated that the more pretreated time used, the more chlorine anion from ILs and H^+ from solid acid were released due to the ion-exchange with the sulfonate (SO₃H) groups, which interacting with the hydroxyl group of cellulose[31] (—SO₃H + [BMIM]Cl →—SO₃ − [BMIM]$^+$+ Cl$^-$+H$^+$). The variation of hydrogen bonds led to decrease the crystalline structure. This result suggested that addition of solid acid catalyst (NR50) could led the pretreated cellulose to obtain the lower M_w value and then make it susceptible to be liquefied in acid-catalyst.[9]

Moreover, irregular cracks were found on the surface of the pretreated cellulose. These alterations were attributed to the breakdown of biomass natural structures, with the disruption of the structure and a reduction in crystalline structure.[32] The surface variation of pretreated cellulose might became more susceptible for acid attack in the subsequent liquefaction process and were supported by liquefied residues result from [Bp]Cl + NR50 sample in Figure 6(b). However, the similar physical chemical properties changes including crystalline structures and M_w distribution were not reflected in the amount of liquefied residues after pretreatment using [B]Cl + NR50.

From the comparison between two ILs [BMIM]Cl and [BMPY]Cl, it was found that the [B]Cl + NR50 sample obtained the lower M_w value of cellulose. The thermal decomposition of sample results suggested that the increase of char residue and degradation temperature indicated the cellulose of larger crystallite size, which was found in [B]Cl + NR50 sample.[26] The fraction of larger sized particles in pretreated cellulose could be attributed to decrease crystalline and M_w value. The M_w distribution suggested that both the lowed M_w and the high M_w value of cellulose have degraded (see Figure 3). Therefore, ILs-water mixtures dissolved the cellulose of lower M_w and the high M_w cellulose changed to loose structure due to the destruction of crystalline structure. Then, the less liquefied residues was obtain by used [B]Cl + NR50 sample compare to that liquefied with [Bp]Cl + NR50 sample (see Figure 6).

In summary, the possible factors causing ILs-water pretreated cellulose can promote liquefied efficiency. First, to understand the reasons of the largest difference result of liquefied residues were occurred in initial phase of liquefaction process in Figure 6, the mechanism of liquefaction process should be discussed. Based on some previous studies,[1,33] cellulose oxygen atoms at both glycosidic bonds and C1 hydroxy of reducing end group due to nucleophilic substitution reaction in the present of acid catalysis, then the derivatives was proposed to proceed. In the end of products, methylene bisphenol and its isomers were found. In this study, FT-IR result showed that the band at 2923 and 2856 cm^{-1} assigned as C—H bending attributed to CH₂ and 1745 cm^{-1}

assigned as C═O bending attributed to ─C(═O)O─. This result obtained on highly substituted cellulose derivatives[34] or glycosidic bond cleavage. However, the largest difference value of liquefied residues (Figure 6) indicated that glycosidic bond cleavage was not support the liquefaction process to be faster. Second, cellulose hydrogen bonding broken could change the intermolecular inter-actions. This is the significant factor to obtain the loose crystal-line structures in cellulose. [B]Cl + NR50 sample and [Bp]Cl + NR50 sample had the similar crystalline structures, but ratio of liquefied residues were different. This result suggests that loose crystalline structures may not be the major factor. Third, both the result of liquefied residues and liquefied products shown that efficient liquefaction process was occurred due to M_w changes of the raw sample. The pretreated sample had lower M_w and larger crystallite size compared with the MCC sample. According to the results, the lower M_w sample obtained the less liquefied residues. However, the result of Mw of liquefied product shows that the pretreatment process may not be intervened to the molecular structure of liquefied products. It is, therefore the efficient liquefaction process was occurred due to the lower M_w of the pretreated sample by ILs-water mixture with solid acid catalysis. The recycles and diversity of ILs-water mixture employed in the pretreatment process will be discussed in future research. It is worth of the forward effective liquefaction reaction and improving energy efficiency of heating process.

REFERENCES

1. Lin, L. Z.; Yao, Y. G.; Yoshida, M.; Shiraishi, N. *Carbohydr. Polym.* **2004**, *57*, 123.

2. Zhao, Y.; Yan, N.; Feng, W. M. *ACS Sustainable Chem. Eng.* **2013**, *1*, 91.

3. Lee, W. J.; Chen, Y. C. *Bioresour. Technol.* **2008**, *99*, 7247.

4. Zhang, Y.C.; Ikeda, A.; Hori, N.; Takemara, A.; Ono, H.; Yamada, T. *Bioresour. Technol.* **2006**, *97*, 313.

5. Kobayashi, M.; Asano, T.; Kajiyama, M.; Tomita, B. *J. Wood. Sci.* **2005**, *51*, 348.

6. Niu, M.; Zhao, G. J.; Alma, M. H. *For. Stud. China.* **2011**, *13*, 71.

7. Pan, H. *Renew. Sust. Energy Rev.* **2011**, *15*, 3454.

8. Yip, J.; Chen, M.; Szeto, Y.S.; Yan, S. *Bioresour. Technol.* **2009**, *100*, 6674.

9. Kobayashi, M.; Asano, T.; Kajiyama, M.; Tomita, B. *J. Wood. Sci.* **2005**, *51*, 348.

10. Earle, M. J.; Seddon, K. R. *Pure. Appl. Chem.* **2000**, *72*, 1391.

11. Swatloski, R. P.; Spear, S. K.; Holbery, J. D.; Rogers, R. D. *J. Am. Chem. Soc.* **2002**, *124*, 4974.

12. Małgorzata, E. Z.; Ewa, B. Ł.; Rafał, B. Ł. *Energy Fuels* **2010**, *24*, 737.

13. Lee, S. H.; Voherty, T. V.; Linhardt, R. J.; Dordick, J. S. *Biotechnol. Bioeng.* **2009**, *102*, 1368.

14. Ha, S. H.; Mai, N. L.; An, G.; Koo, Y. M. *Bioresour. Technol.* **2011**, *102*, 1214.

15. Shill, K.; Padmanabhan, S.; Xin, Q.; Prausnitz, J. M.; Clark, D. S.; Blanch, H. W. *Biotechnol. Bioeng.* **2011**, *108*, 511.

16. Dadi, A. P.; Varanasi, S.; Schall, C. A. *Biotechnol. Bioeng.* **2006**, *95*, 904.

17. Li, Q.; Jiang, X.; He, Y.; Li, L.; Xian, M.; Yang, J. *Appl. Microbiol. Biotechnol.* **2010**, *87*, 117.

18. Kohno, Y.; Ohno. H. *Chem. Commun.* **2012**, *48*, 7119.

19. Rinaldi, R.; Palkovits, R.; Schüth, F. *Angew. Chem. Int. Ed.* **2008**, *47*, 8047.

20. Brandt, A.; Ray, M. J.; To, T. Q.; Leak, D. J.; Murphy, R. J.; Welton, T. *Green. Chem.* **2011**, *13*, 2489.

21. Zhang, Z. Y.; O'Hara, I. M.; Doherty, W. O. S. *Green. Chem.* **2013**, *15*, 431.

22. Cammarata, L.; Kazarian, S. G.; Salterb, P. A.; Welton, T. *Phys. Chem. Chem. Phys.* **2001**, *3*, 5192.

23. Olivier-Bourbigou, H.; Magna, L.; Morvan, D. *Appl. Catal. A* **2010**, *373*, 1.

24. Dadi, A. P.; Varanasi, S.; Schall, C. A. *Biotechnol. Bioeng.* **2006**, *95*, 904.

25. Dadi, A. P.; Schall, C. A.; Varanasi, S. *Appl. Biochem. Biotechnol.* **2007**, *136–140*, *407*.

26. Cheng, G.; Varanasi, P.; Arora, R.; Stavila, V.; Simmons, B. A.; Kent, M. S.; Singh, S. *J. Phys. Chem. B.* **2012**, *116*, 10049.

27. Das, K.; Ray, D.; Bandyopadhyay, N. R.; Sengupta, S. *J. Polym. Environ.* **2010**, *18*, 355.

28. Yamada, T.; Ono, H. *J. Wood Sci.* **2001**, *47*, 458.

29. Bochek, A. M. *Russ. J. Appl. Chem.* **2003**, *76*, 1711.

30. Brandt, A.; Gräsvik, J.; Hallett, J. P; Welton, T. *Green. Chem.* **2013**, *15*, 505.

31. Dwiatmoko, A. A.; Choi, J. W.; Suh, D. J.; Suh, Y. W.; Kung, H. H. *Appl. Catal. A* **2010**, *387*, 209.

32. Tan, H. T.; Lee, K. T.; Mohamed, A. R. *Carbohydr. Polym.* **2011**, *83*, 1862.

33. Sung, P. M.; Jeong, P. J. *J. Ind. Eng. Chem.* **2009**, *15*, 743.

34. Jandura, P.; Kokta, B. V.; Riedl, B. *J. Appl. Polym. Sci.* **2000**, *78*, 1354.